Effect of nitrogen-plasma surface treatment to the enhancement of TiO$_2$ photocatalytic activity under visible light irradiation

Chao-Ming Huang [a,*], Lung-Chuan Chen [b], Kong-Wei Cheng [c], Guan-Ting Pan [a]

[a] *Department of Environmental Engineering, Kun Shan University, Yung Kang City, Tainan 710, Taiwan, ROC*
[b] *Department of Polymer Materials, Kun Shan University, Yung Kang City, Tainan 710, Taiwan, ROC*
[c] *Energy and Environment Laboratory, Industrial Technology Research Institute, Hsin Chu 310, Taiwan, ROC*

Abstract

A visible-light-active commercial TiO$_2$ powder was prepared by thermal nitrogen-plasma processing as the surface treatment. The photoactivity of the treated TiO$_2$ samples was evaluated in the photocatalytic degradation of gaseous 2-Propanol (IPA) in a batch reactor. XPS analysis showed that oxygen vacancies formed in the lattice of the treated TiO$_2$ particles and no nitrogen peaks were detected. With increasing the treating time, the visible absorbance and oxygen vacancies were increased but the surface area of treated sample was decreased. The photodegradation rate of IPA under visible light illumination depended strongly on the treating time of the catalyst, and the photoactivity of the treated sample was higher than that of plain TiO$_2$. From the results of reaction rate constant and mineralization yield of IPA, it was found that the TiO$_2$ powders treated for 30 min demonstrated the highest photocatalytic activity among all samples. This high visible light photoactivity was ascribed to an intermediate level of visible absorbance as well as optimal oxygen vacancies after the thermal nitrogen-plasma surface treatment.
© 2006 Elsevier B.V. All rights reserved.

Keywords: TiO$_2$; Thermal nitrogen-plasma processing; Oxygen vacancies; Mineralization yield

1. Introduction

TiO$_2$ is widely used for the mineralization of environmental pollutants including organic or inorganic and it exhibits strong oxidation activity under ultraviolet light with a wavelength of 390 nm or less. Since ultraviolet (UV) light is only 3–5% part of the solar spectrum, the photocatalytic activity of TiO$_2$ is not enough under the visible and/or solar light irradiation. It would be very valuable to develop visible-light-active TiO$_2$ photocatalysts that can yield efficient reaction under solar light for industrial areas or poor interior lighting illumination in living spaces. In the last decade, the studies of doping TiO$_2$ with different transition metal ions [1,2] to reduce the band gap were intensively investigated, but their efficiency would be reduced due to the formation of electron–hole recombination center. There have recently been a number of reports on non-metal doped-TiO$_2$ with anions of N [3], C [4], and S [5], which caused photo-responses in the visible-light region. Although the visible-light-active pho-

tocatalysis of N-doped TiO$_2$ has been confirmed by many studies, the mechanism of nitrogen that contributes the enhancement of photocatalytic activity remains unclear. For example, Asahi et al. [6] prepared nitrogen doped TiO$_2$ films by sputtering TiO$_2$ in a N$_2$/Ar gas mixture, and then post-annealing at 550 °C in N$_2$ gas for 4 h. From the XPS analysis, they acclaimed three N 1s peaks with binding energies of 402, 400, and 396 eV were observed and concluded that the 396 eV is indispensable for visible-light activity of N-doped TiO$_2$. A similar N-doping of TiO$_2$ film was reported by Yang et al. [7]. They made the TiO$_{2-x}$N$_x$ films by ion-assisted electron-beam evaporation and also found N 1s peaks at 402 and 396 eV. On the other hand, the chemical state for doped N, Sato et al. [8] prepared N-doped TiO$_2$ powders by sol–gel method using titanium tetra-isopropoxide or TiCl$_4$ with aqueous ammonia solution and found only the peak at 400 eV was certainly detected but exhibit no peak at 396 eV. Li et al. [9] studied the N-doped process of TiO$_2$ powders by spray pyrolysis from TiCl$_4$ and different N-precursors; however, the XPS analysis indicated no nitrogen peaks were detected in their samples. In addition, Ihara et al. [10] prepared visible-light active TiO$_2$ powders by the hydrolysis of Ti(SO$_4$)$_2$ with an aqueous ammonia solution and ruled out N-doping to be effective for

---

* Corresponding author. Tel.: +886 6 2050359; fax: +886 6 2050540.
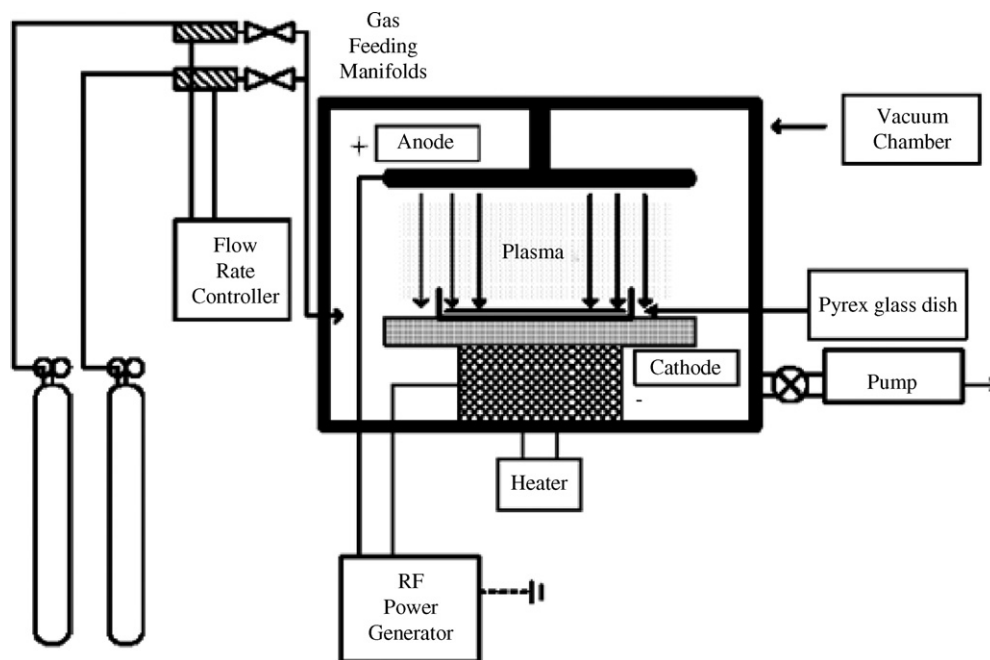*E-mail address:* charming@mail.ksu.edu.tw (C.-M. Huang).

Fig. 1. Scheme of apparatus for plasma surface-treatment over TiO_2 powders.

visible-light activity, since N was a trace amount (0.2%). They concluded that the function of N dopant in TiO_2 was to retard the reoxidation of oxygen-deficient sites which cause visible-light activity. They also confirmed the role of oxygen vacancies in the TiO_2 powders treated with low-temperature H_2 plasma, which is essentially indispensable for visible light sensitization. In view of these results, it is quite obvious that without the bombardment of high-energy nitrogen species, no or very little nitrogen atoms can be incorporated in the TiO_2. Up to date, the contribution of doped nitrogen atoms or oxygen vacancies to the visible-light activity of TiO_2 remains unclear. The relation between the role of oxygen vacancies and the corresponding visible-light-active photocatalytic property has not yet been well investigated. Hence, the purpose of this study is to investigate the variations of photocatalytic properties induced by oxygen vacancies due to the thermal nitrogen-plasma surface treatment. The photocatalytic activities of plain and the plasma-heat treated TiO_2 powders were characterized by 2-Propanol photodegradation under the interior daylight lamp.

2. Experimental

2.1. Materials

The anatase TiO_2 powder (ST-01, Ishihara Sangyo) was chosen as the raw material with the average crystallite size of 6.87 nm determined by X-ray diffraction (XRD). The analytical grade of 2-Propanol was procured from Merck (Germany).

2.2. Preparation of plasma surface-treatment of TiO_2

The surface modification of ST-01 samples were prepared in a stainless steel chamber (12.84 L) with 13.56 MHz radio frequency (RF) power supply (Dressler Hochfrequenztechnik, VM700A) and an automatic impedance matching unit (AMN-100), shown in Fig. 1. The ST-01 powders of 0.5 g were spread out evenly in a Pyrex glass dish and then introduced on the cathode electrode. The chamber was started to vacuum and heating. The temperature of cathode electrode was controlled and monitored with a thermocouple positioned at the backside of the cathode electrode separated from the anode electrode by 3.5 cm. When the chamber was evacuated to a background pressure of 10^{-5} Pa, pure gas of N_2 (99.9995%) was introduced to the chamber. After the pressure and temperature reached to the predetermined values, the plasma was started. Throughout this work, the flow rate of N_2 was kept at constant value of 10 sccm, RF power of 400 W and working pressure at 30 Pa. Conditions for the thermal plasma treatment of powders were investigated by changing treatment period (10–120 min) at 400 °C.

2.3. Analyses of photocatalysts

The crystallinity of TiO_2 samples was verified by XRD (Rigaku DIMAX-2500V/PC, Cu Kα radiation) and their diffraction patterns were measured at an angle of 2θ from 5 to 60°. BET surface area measurements of TiO_2 before and after plasma-heat modifications were carried out by N_2 adsorption at 77 K (Micromeritics ASAP 2020). The surface composition and chemical state of the TiO_2 were examined by X-ray photoelectron spectroscopy (XPS, Omicron Multiprobe Compact) using a monochromatic Al Kα source and the binding energy scale was calibrated to 284.6 eV for C 1s peak. The UV–vis absorbance spectra of raw and treated ST-01 samples were measured by a Hitachi U-3010 spectrophotomer, equipped with an integrating sphere, and a Ba_2SO_4 standard white plate as reference.

2.4. Photocatalytic experiments

0.1 g of TiO_2 powder was uniformly spread over the center of a horizontal Pyrex glass reactor of 1520 cm³ capacity (48 cm height, 8.4 cm i.d.) and was illuminated by a white fluorescent light lamp (TFC, FL10W-EX) or an ultraviolet lamp (PHILIPS, TLD 10 W/08). The light intensity on the surface of powder was 0.2 mW/cm² for visible light and 1.61 mW/cm² for ultraviolet light, respectively. The adsorption and photocatalytic decomposition of gas-phase IPA onto TiO_2 powders were evaluated at room temperature (22 ± 2 °C). Then, liquid IPA was injected into the reactor. Right after vaporization, the IPA samples were withdrawn from a sampling port on the side of the reactor using a microsyringe and injected into the gas chromatograph (Perkin-Elmer, Clarus 500) equipped with a 60 m × 0.53 mm DB-624 capillary column and a thermal conductivity detector to measure the IPA and CO_2 concentrations. The final product of photocatalytic reaction, CO_2, was calibrated using standard CO_2 gas from Supelco Co.

3. Results and discussion

3.1. Characterization comparison of plain and plasma-treated TiO_2

The color of thermal plasma-treated sample was changed from beige to light grey by visible observation depending on the treatment time. The more plasma-heat treatment TiO_2 sample is, the more colored it is. The absorption spectra of TiO_2 samples were shown in Fig. 2. Compared with plain TiO_2, the plasma-heat samples exhibited an obvious absorbance in the visible light region during 400–600 nm. This absorbance increase shifts gradually to higher value as the treating time of powder increases, which implies that thermal RF plasma is an effective technique for the increase of visible light absorption of TiO_2 powders. Several studies [7,9,11] based on nitrogen-doped TiO_2 photocatalysts have been reported that the visible absorption intensity and shift of the absorption shoulder are increased with increasing N-doped concentration. In this study, the shift of the absorption edge of treated TiO_2 was not observed in the visible light region. The XRD diffraction patterns of ST01 before and
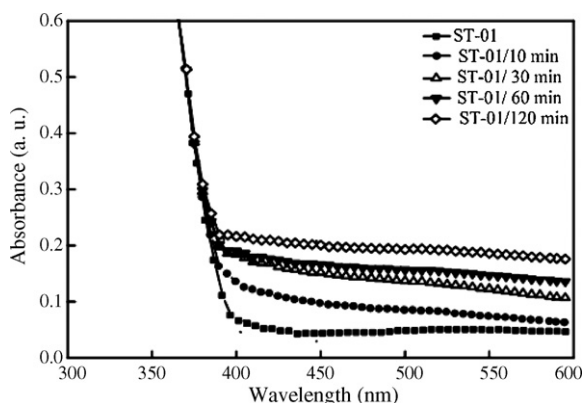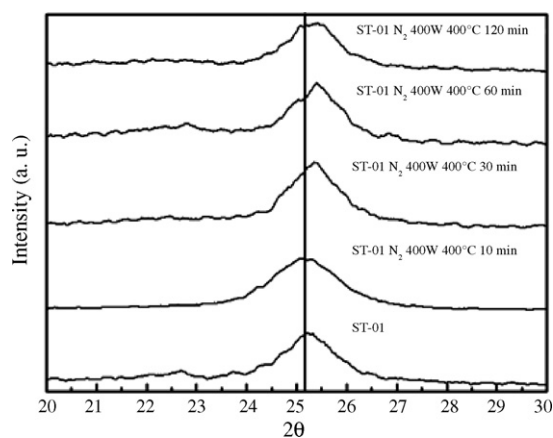

Fig. 3. XRD diffraction patterns of plain and N_2-plasma heat-treated TiO_2 powders.

after plasma-heat treatment indicated that thermal N_2-plasma treatment did not result in any significant phase transfer of ST01. However, the position of the principal (1 0 1) peak shifts gradually to higher diffraction angle with increasing plasma treating time, as shown in Fig. 3. This result implies that oxygen ions are substituted by nitrogen ions, due to the smaller radius of nitrogen ions compared to oxygen ions. The results for surface area measurement and pore structure of TiO_2 powders are shown in Table 1. It can be seen that with increase of treating time leads to the decrease of surface area and the increase of pore diameter, which is attributed to the growth of TiO_2 crystallites due to sintering effect. The founding was different with that of Ihara et al. [12]. They prepared thermal hydrogen plasma treatment of TiO_2 (ST-01) and found that there was no significant change of surface area between the raw and treated ST-01 at 400 °C for 60 min.

3.2. Photoactivity of plain TiO_2 and plasma-treated TiO_2

The photocatalytic decomposition of gaseous IPA was carried out at initial concentration of 25.0 μM. After the adsorption equilibrium of the IPA onto TiO_2 was established (approximately 120 min), the visible light illumination was started. The adsorbed gaseous IPA on a 0.10 g sample at 25 °C was calculated from the difference between the initial and equilibrium concentrations. Fig. 4 shows the adsorption behavior of the IPA over various TiO_2 powders at different treatment conditions. The amount of IPA adsorbed on thermal plasma-treated sample was higher than that of ST-01 and increased with prolonging treating time. The photodegradation of IPA by TiO_2 particles

Fig. 2. Optical absorbance spectra of TiO_2 powders before and after N_2-plasma treatment for different treatment time at 400 °C.

Table 1
Effect of treating time on surface characterizations of TiO_2 powders

Sample	Surface area (m²/g)	Pore volume (nm)	Pore size (nm)
ST-01	323.39	0.59	7.64
ST-01/10 min	313.70	0.58	7.55
ST-01/30 min	294.83	0.57	7.70
ST-01/60 min	276.07	0.55	7.77
ST-01/120 min	261.08	0.56	7.98
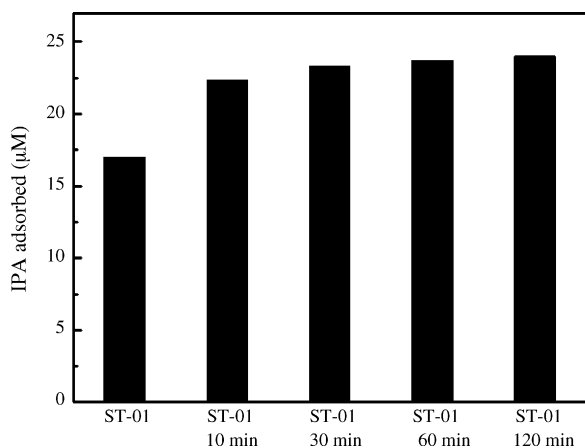
Fig. 4. IPA absorbed on plain and N_2-plasma heat-treated TiO_2 powders.

Table 2
Effect of treating time on apparent rate constant of TiO_2 powders under visible light irradiation

Sample	Apparent rate constant (h^{-1})
ST-01	0.32
ST-01/10 min	1.10
ST-01/30 min	1.27
ST-01/60 min	1.21
ST-01/120 min	1.09

before and after N_2 plasma-heat treatment at 400 °C was shown in Fig. 5. After 100 min of irradiation, the photodecomposition of IPA proceeded to completion when 30 and 60 min plasma-heat treated TiO_2 particles are used, while only 40% of IPA gas has been oxidized using plain TiO_2 during the same time. Also, a longer irradiation time was required for TiO_2 treated over 10 or 120 min. It has been reported that the photocatalytic degradation systems generally follow a Langmuir–Hinshelwood (L–H) kinetic model [13–16], which can be simplified to a pseudo-first-order expression and apparent rate constant can be determined by linear regression of the data $\ln(C_0/C)$ versus the exposure time (t), where C_0 is the initial reaction concentration of the reactant and C is the concentration of the reactant at time t. So, photocatalytic activity of various TiO_2 particles was evaluated by comparing the apparent rate constants. The apparent rate constant of TiO_2 sample under visible irradiation was indicated in Table 2. According the values of apparent rate constant, the following comparisons can be drawn: (1) the photocatalytic activity of TiO_2 powders greatly depends on thermal plasma condition; the maximum activity was observed for TiO_2 powder treated for 30 min, and it was much higher than that of plain TiO_2 and (2) high visible absorption and IPA adsorption could not significantly improve the visible photoactivity, especially for TiO_2 powder treated for 120 min. It can also be noticed
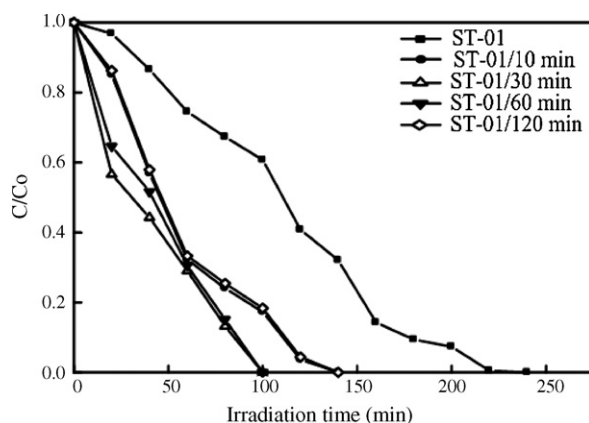
that for this sample (400 °C for 120 min) possesses the lowest surface area (Table 1), but it has the most active surface for the highest light absorption and reactant adsorption, which is probably caused by the formation of new active sites on this treated TiO_2 powder. Similar result was reported by Ihara et al. [10]. They found the TiO_2 containing SO_4^{2-} had specific lowest surface and highest adsorption amount of acetone, but showed no vis-activity under blue-light-emitting diodes illumination. Besides, Li et al. [9] claimed that the visible absorption was directly related to the amount of N-concentration over TiO_2 particles, but only N-doping could not exhibit efficient visible photoactivity. However, the maximum photocatalytic activity was observed for N-F-codoping TiO_2, where F-doping led to the formation of surface acid sites resulting in high adsorptivity and enhanced photoactivity. To identify the chemical states of the TiO_2 powders, XPS analyses were conducted. The XPS results of the TiO_2 samples before and after treatment are shown in Fig. 6. In all samples, the binding energies of Ti ($2p_{3/2}$) and
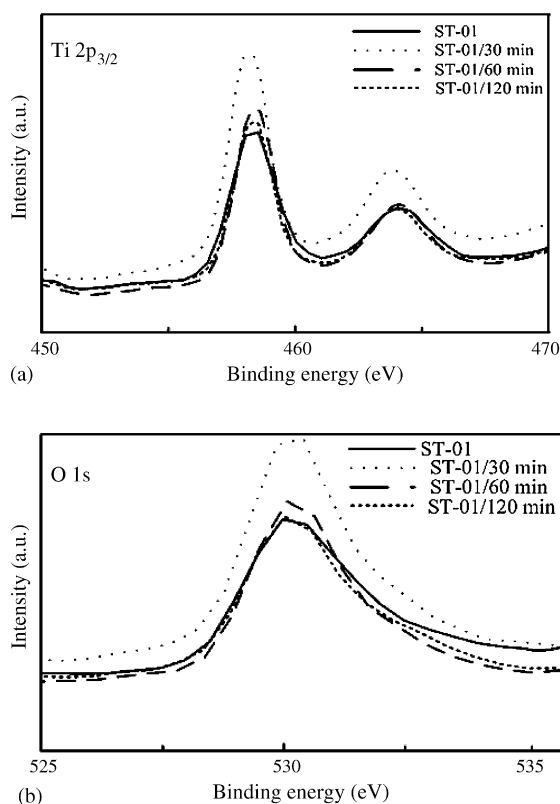

Fig. 5. Photodegradation of IPA (25.00 μM) over plain and N_2-plasma heat-treated TiO_2 powders under visible light irradiation.

Fig. 6. XPS spectrum of (a) Ti $2p_{3/2}$ and (b) O 1s levels for plain and N_2-plasma heat-treated TiO_2 powders.

Table 3
Effect of treating time on the O/Ti ratio of TiO$_2$ powders

Sample	ST-01	ST-01/10 min	ST-01/30 min	ST-01/60 min	ST-01/120 min
O/Ti ratio	2	1.96	1.86	1.84	1.72

Ti ($2p_{1/2}$) are present at 458.5 and 464.2 eV, respectively. The separation between Ti ($2p_{3/2}$) and Ti ($2p_{1/2}$) signals is 5.7 eV, which is consistent with characteristic XPS signals for TiO$_2$ [17]. However, XPS measurements of the treated samples did not show any evidence of the presence of N 1s peaks at 396 or 400 eV in this work. Although the increase in visible-light absorption of TiO$_2$ by N-doping has been confirmed by many studies, the N-doping for improving the visible-light activity is still unclear. Several researchers [8,18,19] acclaimed that N 1s peak at 396 eV was difficult to detect, which is quite different with the reports by Asahi et al. [6] and Yang et al. [7]. On the other hand, Ihara et al. [10] found that the trace amount of N (0.2%) was effective to suppress the reoxidation of the oxygen vacancies of TiO$_2$, which is responsible for visible-light photocatalytic activity. Also, they found out that the new formation of oxygen vacancy state, the sub-band gap level between the valence and the conduction bands of TiO$_2$, was essentially indispensable for the visible light activity of H$_2$-plasma-treated TiO$_2$ [12,20,21]. In order to find the presence and alteration of oxygen vacancies of TiO$_2$ samples in our study, the O:Ti atomic ratios based on XPS spectrum were indicated in Table 3. When treated with thermal N$_2$-plasma, the value of O/Ti ratio decreased as the treating time increased, indicating that the oxygen vacancies are produced in the lattice of the plasma-heat ST-01 particles. It is worth to discuss the interaction between N$_2$ and TiO$_2$ during the thermal N$_2$-plasma treatment. For the treating time, the interaction could be divided into three stages: owing to not enough energy, the relatively weak interaction between nitrogen molecules and TiO$_2$ resulted in a little change of O/Ti ratio at the sample treated for 10 min; as the treating time was increased to 30 and 60 min, the heating energy was enough to excite the TiO$_2$ and nitrogen atoms interacted effectively with the O atoms in the lattice of TiO$_2$, which cause the formation of oxygen vacancies; In the case of 120 min, more energy was supplied and the interaction between nitrogen molecules and TiO$_2$ was drastic, which led to the obvious increase of the oxygen vacancies. Compared the experimental results with oxygen vacancies, it can be seen that further increase of oxygen vacancies leads to the increase of visible absorption, but photoactivity of treated TiO$_2$ decreases as the oxygen vacancies increased. For the visible absorption, it might be due to the Ti^{3+} effect stated by Ishigaki et al. [22]. They pointed out that the formation of Ti^{3+} was related to color change of TiO$_2$, while the color was white or beige if the concentration of Ti^{3+} was low. In our study, the unique non-equilibrium situation of plasma and the time-dependent of heating are able to make the electrons already in the oxygen vacancies be driven and transferred to Ti^{4+}, which results in the generation of Ti^{3+}. Therefore, the more oxygen vacancies were produced as a result of the greater introduction of Ti^{3+} in its structure when the treating time was increased.
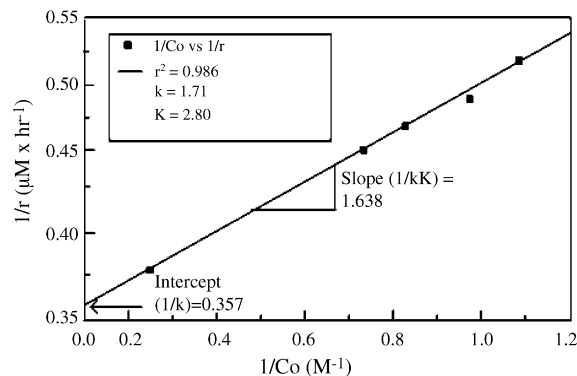

Fig. 7. Linearized plot of $1/r_{IPA}$ against $1/C_{IPA}$ for N$_2$-plasma heat (400 °C for 30 min) treated TiO$_2$.

This explained why the visible absorption was higher as oxygen vacancies increased.

Since the oxygen vacancies of TiO$_2$ samples treated for 30 and 60 min were very close, these two samples were chosen to further investigate the effect of treating time on the photocatalytic degradation rate in more detail. Kinetic analysis based on the L–H kinetics model was carried out from Eq. (1).

$$r_0 = \frac{kKC_0}{1 + KC_0} \text{ or } \frac{1}{r_0} = \frac{1}{kK}\frac{1}{C_0} + \frac{1}{k} \tag{1}$$

where r_0 is initial photocatalytic degradation rate ($\mu M \times h^{-1}$), C_0 the initial reaction concentration of IPA (μM), k the reaction rate constant ($\mu M \times h^{-1}$) and K is the Langmuir adsorption constant (μM^{-1}).

A linear plot of $1/r_0$ versus $1/C_0$ was obtained with regression coefficient greater than 0.985 in this work. Fig. 7 shows plot of the reciprocal of the initial reaction rate versus the reciprocal of the five initial reaction levels of IPA. The kinetic parameters k and K were obtained from the intercept and slope of the straight line, respectively. Table 4 showed the dependence of treating time on reaction rate constant and adsorption constant. For TiO$_2$ samples treated for 30 and 60 min, the values of k and K were higher than those of plain TiO$_2$, especially for K. Some recent researches [21] confirmed that oxygen vacancies help in the trapping of photogenerated electrons, thus limiting the electron–hole recombination, which contributed to the

Table 4
Effect of treating time on reaction rate constant (k) and adsorption constant (K) of TiO$_2$ powders under visible light irradiation

Sample	k ($\mu M \times h^{-1}$)	K ($\mu M \times h^{-1}$)
ST-01	1.98	0.80
ST-01/30 min	2.80	1.71
ST-01/60 min	2.64	1.78

Table 5
Mineralization of plain and N_2-plasma heat-treated TiO_2 powders after 720 min of visible (VIS) or ultraviolet (UV) light irradiation

Sample	VIS-irradiation (%)	UV-irradiation (%)
ST-01	39.9	70.9
ST-01/10 min	78.7	–
ST-01/30 min	97.8	78.3
ST-01/60 min	80.8	76.7
ST-01/120 min	68.4	–

enhancement of photocatalytic activity. However, it must be taken into account that too much oxygen vacancies could act as recombination centers for electron–hole pairs [23], although the TiO_2 treated for 120 min exhibited the most oxygen vacancies but the lowest photoactivity. To determine the durability of treated sample in photocatalytic activity, the TiO_2 treated for 30 min stored at room temperature after 2 months was also examined by kinetic analysis. The value of k and K was 2.55 and 1.66, respectively. Fortunately, the result indicted that there was only a slight decrease as compared to the freshly treated TiO_2 powder.

In order to clarify the role of oxygen vacancies of treated TiO_2 in the photocatalytic reaction, the experiments of the mineralization yield of gaseous IPA under two different light sources (fluorescent light lamp and ultraviolet lamp) were conducted for three samples, such as the plain and treated for 30 and 60 min TiO_2. The mineralization yield of gaseous IPA is defined as follows [24]:

$$\text{mineralization} \, (\%) = \frac{1/3[CO_2]_{production}}{[CH_3CHOHCH_3]_{original}} \times 100\%$$

When 100% mineralization yield occurs, 3 mol of carbon dioxide are formed from each mole of IPA. The results of mineralization yield after 720 min of visible or ultraviolet light illumination were listed in Table 5. The plain ST-01 revealed high photocatalytic activity under UV irradiation, while it showed slightly considerable mineralization yield in visible light. In this study, ST-01 is still visible-light-active, since the illumination of white fluorescent light lamp is comprised of about 3–5% ultraviolet light. The TiO_2 samples treated for 30 and 60 min exhibited high activity in both UV and visible light, and the mineralization yield in visible light was discernible higher than that of in UV. These results confirm that these two treated TiO_2 were more visible-light-active compared to plain ST-01 under visible light illumination, due to the formation of oxygen vacancies induced by the thermal N_2-plasma surface treatment. As can be seen from Fig. 2, TiO_2 treated for 120 min showed the highest absorption in visible light region. However, this catalyst has lowest mineralization yield among the treated samples. Thus, it is concluded that enhanced absorption of visible light is a necessary condition but not a sufficient condition for the visible-light-active photocatalyst. As mentioned above, the TiO_2 treated for 30 min had the highest reaction rate constant as well as CO_2 formation. It can also be noticed that an intermediate level of visible-light absorption level combined with optimum structure defects (oxygen vacancies)

render the TiO_2 treated for 30 min the highest photocatalytic activity.

4. Conclusions

The visible-light-photoactive TiO_2 powders were prepared by thermal N_2-plasma treatment at RF power of 400 W and the heating temperature of 400 °C for the different treating periods. The treating time greatly influenced the visible light absorption, BET surface, IPA adsorption and photocatalytic activity of the prepared TiO_2 samples. The XPS results showed that during the N_2-plasma surface treatment, the oxygen vacancies were produced and attributed to the increase of visible absorbance and the enhancement of photocatalytic activity. For powders treated for 30 min, the photocatalytic activity of TiO_2 exhibited the highest photoactivity with an intermediate level of visible-light absorption level as well as optimum oxygen vacancies. The thermal N_2-plasma method was proved to modify the surface of TiO_2 by means of the introduction of oxygen vacancies and the experimental results confirmed the enhanced photocatalytic activities of treated TiO_2 were not the contribution of doped nitrogen atoms but the oxygen vacancies.

References

[1] T. Lòpez, R. Gòmez, G. Pecci, P. Reyes, X. Bokhimi, O. Novaro, Mater. Lett. 40 (1999) 59–65.
[2] J. Engweiler, J. Harf, A. Baiker, J. Catal. 159 (1996) 259–269.
[3] V. Pore, M. Heikkila, M. Ritala, M. Leskela, S. Areva, J. Photochem. Photobiol. A: Chem. 177 (2006) 68–75.
[4] S.U.M. Khan, M. Al-Shahry, W.B. Ingler Jr., Science 297 (2002) 2243–2245.
[5] T. Ohno, M. Akiyoshi, T. Umebayashi, K. Asai, T. Mitsui, M. Matsumura, Appl. Catal. A: Gen. 265 (2004) 115–121.
[6] R. Asahi, T. Morikawa, T. Ohwaki, K. Aoki, Y. Taga, Science 293 (2001) 269–274.
[7] M.C. Yang, T.S. Yang, M.S. Wong, Thin Solid Films 469–470 (2004) 1–5.
[8] S. Sato, R. Nakamura, S. Abe, Appl. Catal. A: Gen. 284 (2005) 131–137.
[9] D. Li, H. Haneda, S. Hishita, N. Ohashi, Mater. Sci. Eng. B: Solid 117 (2005) 67–75.
[10] T. Ihara, M. Miyoshi, Y. Iriyama, O. Matsumoto, S. Sugihara, Appl. Catal. B: Environ. 42 (2003) 403–409.
[11] H. Irie, Y. Watanabe, K. Hashimoto, J. Phys. Chem. B 107 (2003) 5483–5486.
[12] T. Ihara, M. Miyoshi, M. Ando, S. Sugihara, Y. Iriama, J. Mater. Sci. 36 (2001) 4201–4207.
[13] W.Z. Tang, H. An, Chemosphere 31 (1995) 4157–4170.
[14] A.M. Peiró, J.A. Ayllón, J. Peral, X. Doménech, Appl. Catal. B: Environ. 30 (2001) 359–373.
[15] A. Bouzaza, A. Laplancheb, J. Photochem. Photobiol. A: Chem. 150 (2002) 207–212.
[16] S.B. Kim, S.C. Hong, Appl. Catal. B: Environ. 35 (2002) 305–315.
[17] E. McCafferty, J.P. Wightman, Surf. Interface Anal. 26 (1998) 549–564.
[18] Y. Sakatani, J. Nunoshige, H. Ando, Chem. Lett. 32 (2003) 1156–1157.

[19] J.L. Gole, J.D. Stout, C. Burda, Y. Lou, X. Chen, J. Phys. Chem. B 108 (2004) 1230–1240.

[20] K. Takeuchi, I. Nakamura, O. Matsumoto, S. Sugihara, M. Ando, T. Ihara, Chem. Lett. (2000) 1354–1355.

[21] I. Nakamura, N. Negishi, S. Ktusuna, T. Ihara, S. Sugihara, K. Takeuchi, J. Mol. Catal A: Chem. 161 (2000) 205–212.

[22] T. Ishigaki, H. Haneda, N. Okada, S. Ito, Thin Solid Films 390 (2001) 20–25.

[23] H. Irie, Y. Watanabe, K. Hashimoto, J. Phys. Chem. B 107 (2003) 5483–5486.

[24] X. Fu, W.A. Zeltner, M.A. Anderson, Appl. Catal. B: Environ. 6 (1995) 209–224.